Angular distribution of product internal states using laser fluorescence detection: The Ba+KCl reaction

Gregory P. Smith and Richard N. Zare

Department of Chemistry, Columbia University, New York, New York 10027
(Received 28 October 1975)

The gas-phase reaction Ba + KCl →BaCl + K has been investigated under crossed beam conditions using laser fluorescence detection of the BaCl and K products. The angular distributions of individual BaCl vibrational states have been obtained. For low v, forward and backward peaks are observed; for high v, insufficient product translational energy is present to resolve separate peaks; and for all v, approximately 58% of the BaCl product is forward scattered. The reaction is interpreted as proceeding through an osculating complex. Although this complex is estimated to live one-half of a revolution, the energy partitioning is decidedly nonrandom. The peak of the vibrational product population occurs near $v = 7$, and considerable rotational excitation is present.

I. INTRODUCTION

Previously, almost all angular distributions of the products formed in bimolecular reactions have been measured by classical molecular beam techniques.[1] Here the product molecules at a given angle relative to the reactant beams are velocity selected and then detected by hot-wire surface ionization or by electron impact ionization, followed by mass analysis. Data thus collected enable one to construct a contour map showing the distribution of product molecules as a function of laboratory angle and velocity. This distribution is then transformed to the center-of-mass coordinate system. The information therein on energy partitioning in the products and on the direction of final product motion provides clues to the reaction mechanism and data for comparison with theoretical models.

We have utilized a different detection technique, laser-induced fluorescence (LIF),[2] in a crossed beam study of the reaction

$$\mathrm{Ba + KCl \rightarrow BaCl + K} \quad \Delta H = -9.5 \pm 3.5\ \mathrm{kcal/mole}. \qquad (1)$$

The exothermicity in Eq. (1) is based on the known dissociation energies of KCl[3] and BaCl.[4] Ground state BaCl product molecules in a particular vibrational–rotational level (v, J) are excited by light of a given wavelength from a tunable dye laser to a given level (v', J') of an excited state. These excited molecules then fluoresce to a variety of (v'', J'') levels of the ground state, and a fraction of this fluorescence is detected by a photomultiplier. The observed fluorescence signal is proportional to the number of BaCl molecules produced initially in the (v, J) level. By measuring the fluorescence intensity as a function of angle and excitation wavelength, we can obtain extensive information on the recoil directions of product molecules in given internal states, and the division of energy among the degrees of freedom of the products.

In contrast to more usual detection techniques, LIF can provide very detailed internal state distributions for both vibration and rotation. Past crossed-beam studies have yielded vibrational distributions of products only in very rare cases of suitable mass combinations[5] or when one of the reaction products is a highly polar salt molecule so that its electric resonance spectrum can be utilized.[2] However, just as the use of a velocity selector cannot provide accurate internal energy distributions, LIF cannot give an accurate velocity distribution, unless the spread in reactant beam energies is appreciably narrowed. This improvement, i.e., the addition of a velocity selector to LIF, awaits future experimental advances. Still, it should be noted, the energy resolution afforded by LIF internal state distributions is much higher than that from velocity distributions obtained by conventional methods. In contrast to electron impact ionization detection, LIF detection is not universal, but instead is limited to small molecules with nonpredissociative transitions that can be excited by presently available lasers.

Previous LIF studies[2] of reactions have concentrated on the measurement of product internal state distributions. This has been accomplished using either a beam-gas arrangement or a crossed-beam arrangement in which the laser beam passes through the reaction zone. In both cases, directional information available in crossed-beam studies is absent. One angular distribution using the LIF technique has been reported[4] for the thermoneutral reaction

$$\mathrm{Ba + LiCl \rightarrow BaCl + Li} \quad \Delta H = +1.0 \pm 3.0\ \mathrm{kcal/mole}. \qquad (2)$$

Since the light lithium atom must have most of the center-of-mass velocity, the BaCl product is constrained kinematically to lie at angles close to the center of mass. Consequently, the question of whether a long-lived intermediate complex is formed remains unanswered. Reaction (1) is an analogous alkaline earth–alkali halide exchange reaction, featuring a much more favorable mass combination. The resulting angular spread makes the BaCl product less dense and its detection more difficult.

Reactions (1) and (2) are quite similar to the well-studied alkali metal–alkali halide exchange reactions,[6,7] such as K + RbCl → KCl + Rb. Products from this reaction show systematic forward–backward peaking at 0° and 180° in the center-of-mass system, indicative of a long-lived collision complex. More exothermic reactions of this family, such as those between Li and the potassium halides, are described by shorter-lived osculating complexes, or direct spectator stripping reactive

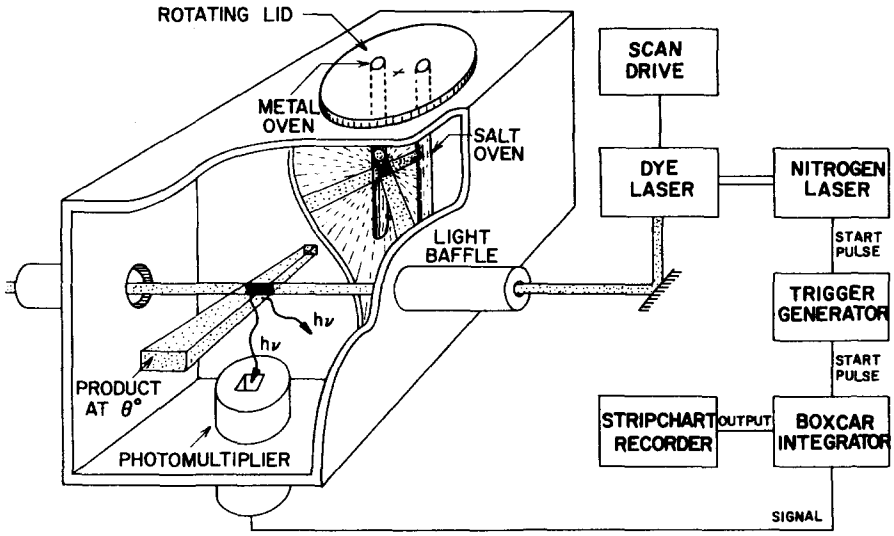

FIG. 1. Schematic representation (partial cutaway) of the experimental apparatus. The beam sources are mounted perpendicular to each other on a rotating lid (beam collimators are not shown for simplicity). Only product molecules at an angle θ from the Ba beam are allowed to enter the laser detection region. By changing the angle θ and by scanning the laser wavelength, product angular distributions of individual internal states are obtained.

events. Reaction (1) differs only in the substitution of an alkaline earth atom for an alkali atom. Consequently, it presents the opportunity to explore the energy partitioning and collision dynamics of this class of reactions in which the reaction intermediate ranges from direct to long lived.

II. EXPERIMENTAL

The experimental apparatus, shown in Fig. 1, does not differ significantly from that used earlier.[4] Two beam ovens are mounted at right angles on a rotatable lid. Only products formed at the angle θ are allowed into the detection region. The scattering angle θ can be varied from $-20°$ to $110°$ where θ is measured from the Ba beam to the KCl beam. The Ba beam has a width of 4° FWHM and a temperature of 1250° K, while the KCl beam is 10° FWHM at 1050° K and contains ~10% dimers.[3] Note that the reaction of Ba with $(KCl)_2$ is highly endothermic. At these temperatures, product molecules are formed in the reaction zone at the upper limit of single-collision conditions. High intensity is needed here for sufficient product signal. The detector slit has a 3° acceptance angle. The excitation zone is a 0.2 cm diameter laser beam in the plane of scattering 22 cm from the collision region. Fluorescence is detected by a photomultiplier (RCA 7265, 2 in. diam S-20 photocathode) mounted directly beneath the excitation zone. A boxcar integrator samples the output for 50 nsec immediately following the laser pulse, and averages the signal using a 5 μsec time constant. The laser wavelength is swept at ~2.5 Å/min.

The dye laser is a Molectron model DL-400 pumped by a pulsed nitrogen laser (Molectron UV-300). The laser is pulsed at 10 Hz and produces a bandwidth of ~0.25 Å. The dye is a mixture of CSA-22[8] with coumarin 1 which covers the spectral range 500–535 nm. The laser is operated at full power, resulting in limited optical pumping[9] of some levels of BaCl. However, measurements indicate the resulting error in populations from such nonlinearities to be comparable to beam and laser fluctuations (~5%).

We have examined the LIF spectrum[10] of BaCl from Reaction (1) using the BaCl $(C\,^2\Pi_{3/2}-X\,^2\Sigma^+)$ $\Delta v = 0$ sequence of red-shaded bands between 5110–5160 Å. Since the X and C potential curves almost parallel each other, the band heads are very close, and most of the intensity for this transition, in absorption and fluorescence, is concentrated in these bands. As a result, the relative populations in the v_1 and v_2 levels are given simply by the approximation[11]

$$\frac{N(v_1)}{N(v_2)} = \frac{I(v_1, v_1)}{I(v_2, v_2)} \frac{q_{v_2 v_2}}{q_{v_1 v_1}} , \tag{3}$$

where $q_{v'v}$ is the Franck–Condon factor for the $(v',\ v)$ transition, and $I(v',\ v)$ is the total fluorescence intensity for all rotational lines in the $(v',\ v)$ band. Unfortunately, the band heads are close in position and many rotational lines of higher vibrational levels contribute to the intensity at the wavelength of a given band head. The crowded and unresolved rotational structure inhibits the analysis of the product rotational energy distribution, but such a compact spectrum also boosts the intensity of the LIF signal for difficult experiments, as is the case here.

III. RESULTS

Figure 2 shows two BaCl excitation spectra taken at different angles. The 30° angle is roughly at the center of mass, while 55° is more in the direction of the KCl beam. In each case, the R_2 vibrational band heads formed around $J = 60$ for all v are barely discernible. In addition, a long tail extends to 5160 Å. This suggests a high degree of rotational excitation. Note also that vibrational (see left side of Fig. 2) and rotational (see right side of Fig. 2) excitation decreases at angles further from the center of mass. Results at 10° (near the direction of the Ba beam) are similar to those at 55°. The heights of these raw spectra are scaled to each other by comparing the intensity of the (0, 0) band head (5140 Å) at different scattering angles. Populations beyond $v = 18$ are extremely difficult to estimate with the $\Delta v = 0$ sequence due to the appearance of a large unidentified spectral feature. Instead, the weaker Δv

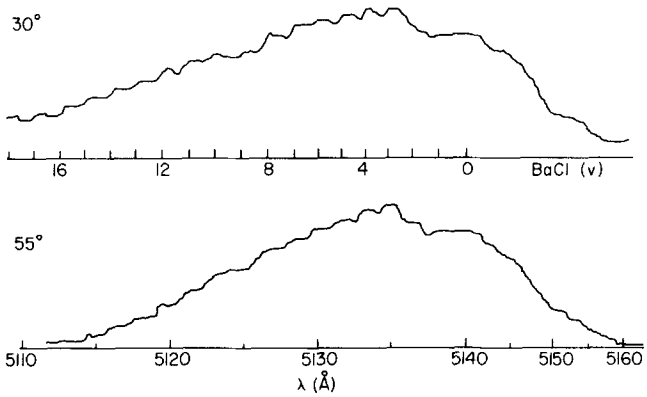

FIG. 2. BaCl excitation spectra for the two scattering angles $\theta = 30°$ (near the center-of-mass angle) and $\theta = 55°$ (backward scattered, toward the KCl beam). The $\Delta v = 0$ sequence of the BaCl $C\,^2\Pi_{3/2} - X\,^2\Sigma^+$ band system is shown. Two horizontal scales are given and apply to both scattering angles, one marking the (v, v) band heads, the other the wavelength (which has a scale change to the red of 5140 Å). Note that the heights of the (v, v) band heads for large v are reduced at $\theta = 55°$ compared to $\theta = 30°$.

$= -1$ sequence is examined by making the excitation zone coincide with the reaction zone. It is found that the intensity of product signal drops off sharply for $v = 19$ and 20, the highest detected levels.

While even such poorly resolved spectra present a good qualitative view of the reaction, a quantitative determination of vibrational populations requires least squares simulation of the spectra. An attempt was made to rotationally relax the spectra using a variety of gases in the detector region. While this sharpened the appearance of the band heads, it also caused significant vibrational relaxation, and thus could not be used to simplify the vibrational population analysis.

Lacking more refined data, we have chosen Boltzmann distributions to represent rotational populations. Since even high vibrational levels at large angles show no sharp band heads, all rotational temperatures must exceed ~1000 °K. We also assume that rotational temperatures for high vibrational levels are lower since less energy is available. The following procedure is used to obtain a rotational temperature for the $v = 0$ level at each angle. Vibrational intensities of the first five levels are equated to band head heights, and the rotational temperatures are assumed equal. A least squares fit is then made of the spectrum in the region 5140–5160 Å to find the best value of T_{ROT}. This produces a satisfactory fit, clearly distinguishable within 400° intervals. For $\theta = -10°$ and 67°, $T_{\mathrm{ROT}}(v = 0, \theta) \approx 1600$ °K; for $\theta = 10°$ and 55°, $T_{\mathrm{ROT}}(0, \theta) \approx 4000$ °K; and for $\theta = 20°$, 30°, and 40°, $T_{\mathrm{ROT}}(0, \theta) \approx 5200$ °K.

To estimate the value of T_{ROT} at the highest v level populated, two procedures are used. First, $T_{\mathrm{ROT}}(20, \theta)$ is set equal to 1000 °K plus three-quarters of the difference $T_{\mathrm{ROT}}(0, \theta) - 1000$. Second, $T_{\mathrm{ROT}}(20, \theta)$ is set equal to 1000 °K plus one-quarter of the difference $T_{\mathrm{ROT}}(0, \theta) - 1000$. Finally, the values of T_{ROT} for intermediate vibrational levels are found by linear interpolation between $T_{\mathrm{ROT}}(0, \theta)$ and $T_{\mathrm{ROT}}(20, \theta)$. Mathematically,

$$T_{\mathrm{ROT}}(v, \theta, \pm) = (20 - v)\, T_{\mathrm{ROT}}(0, \theta) + v[\tfrac{1}{2} T_{\mathrm{ROT}}(0, \theta) + 500 \pm \tfrac{1}{4}(T_{\mathrm{ROT}}(0, \theta) - 1000)]. \quad (4)$$

The computer simulation of a spectrum utilizes the following (unnormalized) intensity of a vibrational–rotational level:

$$I(\theta, v, J) = I_0(\theta, v)[1 - (20 - v)c]J \times \exp[-BJ^2/kT_{\mathrm{ROT}}(v, \theta, \pm)]/T_{\mathrm{ROT}}(v, \theta, \pm). \quad (5)$$

Here, I_0 is the intensity at the v band head and c is the parameter varied. Thus, the simulated vibrational intensities correspond to a linear scaling of the original band head intensity measurements. This is a crude but reasonable procedure since the (0, 0) band head has more contributions from higher vibrational states than do the higher vibrational band heads.

This procedure produces a good fit to the observed spectra for specific c; hence, vibrational populations can be determined with some degree of accuracy. Both the high and low sets of rotational temperatures [corresponding to the ± sign in Eq. (4)] give satisfactory fits. Thus, a crude estimate of rotational populations would be quite imprecise.

Once the intensities at the band heads are corrected for rotational background contributions, the angular distributions of the different vibrational levels are obtained using Eq. (3). Morse Franck–Condon factors can easily be calculated[10] with sufficient accuracy for this analysis. Finally, we must convert from number density to flux, since LIF determines concentrations. This correction is made by multiplying the number density by the appropriate laboratory velocity, $\mathbf{v}_{\mathrm{LAB}}$. The product translational energy must equal the total energy minus the BaCl internal energy. However, the distribution of reactant energies that produces a given internal state at a given angle is unknown, and this causes the center-of-mass translational energy to be uncertain. Moreover, $\mathbf{v}_{\mathrm{LAB}}$ may be expected to vary with angle. Its uncertainty is a major liability in the use of LIF for quantitative crossed-beam work.

Figure 3 shows a Newton diagram for the Ba + KCl reaction. This sketch of velocity vectors illustrates the difficulty in deducing the distribution of laboratory velocities, $\mathbf{v}_{\mathrm{LAB}}$, from the angular distribution of the products alone. In Fig. 3 $\mathbf{v}_{\mathrm{c.m.}}$ and $\mathbf{v}_{\mathrm{REL}}$ are the center of mass and relative velocity vectors, respectively, of the colliding reactants. The circle, labeled U and centered about the tip of $\mathbf{v}_{\mathrm{c.m.}}$ gives the possible locus of all velocity vectors u in the center-of-mass reference system corresponding to BaCl products having a given translational (and internal) energy. The angular distribution of BaCl products in a certain internal state is measured in the laboratory reference frame. Let θ denote the laboratory scattering angle measured from the Ba beam direction toward the KCl beam direction. As Fig. 3 illustrates, there are in general two different laboratory velocities, $\mathbf{v}_<$ (LAB) and $\mathbf{v}_>$ (LAB), associated with each laboratory scattering angle θ. Conversion of product density to product flux, which is the kinetically meaningful quantity, requires a knowledge

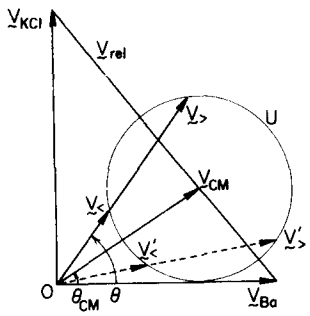

FIG. 3. Newton diagram for the Ba + KCl reaction. The vectors v_{Ba} and v_{KCl} represent the most probable reactant beam velocities. The point 0 is the origin of the laboratory coordinate system. The relative velocity vector v_{REL} and the center-of-mass velocity vector $v_{c.m.}$ at the laboratory angle $\theta_{c.m.}$ are also shown. The angle θ, measured from the Ba beam, represents the laboratory scattering angle. The circle U is the locus of all possible product velocity vectors $\mathbf{u}$ in the center-of-mass coordinate system. The figure shows that to each u and θ corresponds two laboratory velocity vectors $v_<$ and $v_>$. Note that $v_{c.m}$ is almost perpendicular to v_{REL}. Consequently, for scattering angles symmetrically placed about $\theta_{c.m}$, the corresponding lengths of $v_<$ and $v_>$ are nearly the same (see dashed line).

or estimate of the relative contributions of $v_<$ (LAB) and $v_>$ (LAB) for each angle θ. This calculation is unfortunately further complicated by the spread in $\mathbf{v}_{c.m.}$ and $\theta_{c.m.}$ caused by the distribution of the vectors $\mathbf{v}_{KCl}$ and $\mathbf{v}_{Ba}$. However, this situation may be handled by computer simulation. Here one assumes a functional form of the center-of-mass product intensity distribution, expressed in terms of the center-of-mass scattering angle Θ and velocity u, and containing adjustable parameters. Then, various possible laboratory angular distributions are calculated, where in each case the appropriate averages over the initial beam conditions are performed. By comparing the calculated laboratory angular distribution to the measured one, the parameters in the center-of-mass product distribution are fixed. This permits us to carry out the density-to-flux transformation and to obtain an estimate of the product translational energy for each vibrational level.

The kinematics of the Ba + KCl reaction are rather favorable in that this transformation will not distort appreciably the observed angular distribution. As seen in Fig. 3, $\mathbf{v}_{c.m.}$ is nearly perpendicular (86°) to $\mathbf{v}_{REL}$. As a consequence, the detector scans nearly equivalent portions of center-of-mass velocity space forward and backward of the center of mass angle $\theta_{c.m.}$ This is shown in Fig. 3 by the velocity vector $\mathbf{v}'_{LAB}$ (dashed line) which is symmetrical to $\mathbf{v}_{LAB}$ about $\mathbf{v}_{c.m.}$ Note that $v_<$(LAB) and $v_>$(LAB) have almost the same values as $v'_<$(LAB) and $v'_>$(LAB). This symmetry implies that reaction products produced from a persistent complex, an intermediate living several rotational periods, must show equal forward and backward peaking in the laboratory product distribution, whether or not the transformation from density to flux is made. Thus, while the density-to-flux transformation can alter the form of the angular distribution, it does so in a manner such that angles symmetrically placed about $\theta_{c.m.}$ are similarly affected.

The following procedure is used in the computer simulation. The center-of-mass product distribution is assumed to separate into a product of two factors, one of which depends only on the velocity u, the other on the angle Θ:

$$I_{c.m.}(u, \Theta) = T(u) A(\Theta) \ . \tag{6}$$

The form of velocity factor $T(u)$ is chosen to be a convex parabola with a full width of 3×10^3 cm/sec:

$$T(u) = -(u - u_p + 1.5\times10^3)(u - u_p - 1.5\times10^3), \tag{7}$$

where u_p is the velocity corresponding to the peak intensity. The form of the angular factor $A(\Theta)$ is chosen to represent the exponential decay of a prolate top[6]

$$A(\Theta) = (\sin\Theta)^{-1} \sum_{n=0}^{\infty} \{\exp[-(\Theta + 2\pi n)/2\pi\tau] + \exp[-(2\pi - \Theta + 2\pi n)/2\pi\tau]\} \ . \tag{8}$$

Here the first exponential expresses the decay of those complexes rotating from 0 to Θ and the second exponential the decay of those rotating in the opposite direction from 0 to $2\pi - \theta$. The origin of the $(\sin\Theta)^{-1}$ factor has the same explanation as the reason why the intersections of the longitudes and latitudes on a globe are more bunched at the poles and spread out at the equator. The constant τ measures the average lifetime of the complex in units of rotational periods. We define $\Theta = 0$ as along the direction $\mathbf{v}_{c.m.} - \mathbf{v}_{Ba}$ (i.e., along $\mathbf{v}_{REL}$).

The laboratory coordinates v, θ corresponding to u, Θ are determined for the various positions and magnitudes of $\mathbf{v}_{c.m.}$ arising from the spreads in the reactant beams. In this manner, an average is taken over the beam velocity distributions, which are assumed to be effusive. The product intensities (fluxes) $I_{c.m.}(v, \theta) = I_{c.m.}(u, \Theta)$ are then transformed to laboratory frame densities by using the appropriate Jacobian factor[12] to obtain

$$D_{LAB}(\theta) = \sum_v \left(\frac{1}{v}\right)\left(\frac{v}{u}\right)^2 I_{c.m.}(v, \theta). \tag{9}$$

This transformation can be seen to weight more heavily $I_{c.m.}(v_>, \theta)$ than $I_{c.m.}(v_<, \theta)$.

Figure 4 shows the best fits obtained by this procedure. The constant τ used for the center-of-mass angular distribution is 0.5, corresponding to a lifetime of one-half of a rotation. Thus, both experimental and simulated angular distributions of BaCl product densities show ~58% of the intensity is forward scattered ($\theta < \theta_{c.m.}$). The average values of u used for the vibrational levels $v = 15$, 10, 5, and 0 are, respectively, 1.5×10^3, 7.5×10^3, 1.15×10^4, and 1.75×10^4 cm/sec. The simulated distributions fit the data points quite well, but still can only be considered approximate and nonunique estimates of the actual distributions. The velocity peaks and widths may vary by roughly 1.5×10^3 and 2.0×10^3 cm/sec, respectively, and the lifetime constant τ may vary from 0.3 to 0.9. Many other functions may also succeed, including some not separable into angular and velocity factors. Nonetheless,

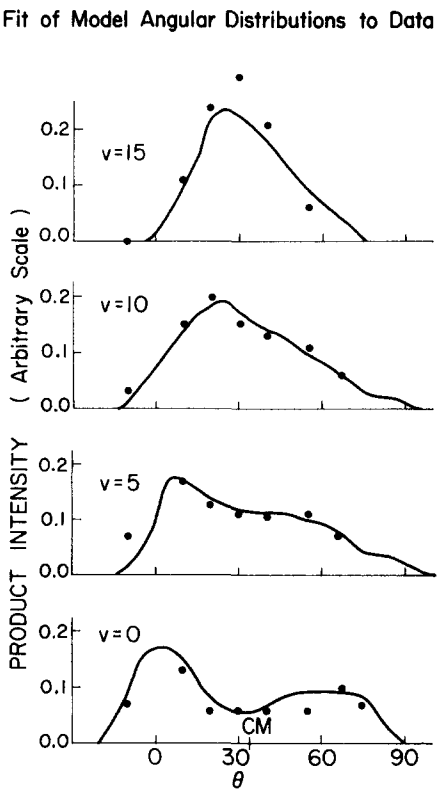

FIG. 4. The BaCl product density distribution of selected v levels as a function of the scattering angle θ. The closed circles are the experimental data and the solid curves are the best fit using the model of an exponentially decaying prolate complex ($\tau = \frac{1}{2}$ revolution).

the present results are sufficient to enable reliable conclusions to be drawn from the measured angular distributions.

Figure 5 is a graph of relative vibrational populations (densities) as a function of laboratory angle for several

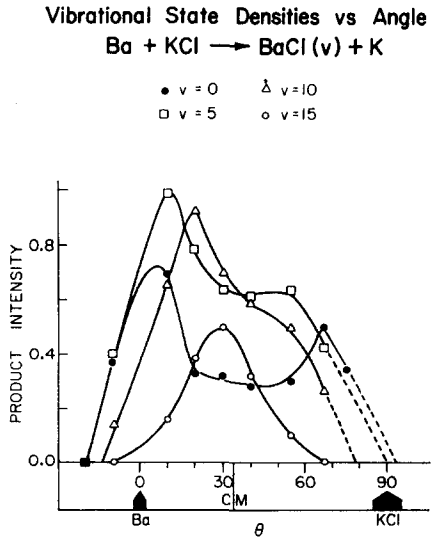

FIG. 5. Plot of the BaCl vibrational state densities as a function of the laboratory scattering angle θ. The angular widths of the reactant beams are indicated. Curves connect the experimental points to aid visualization. The figure reflects the relative populations of the vibrational levels.

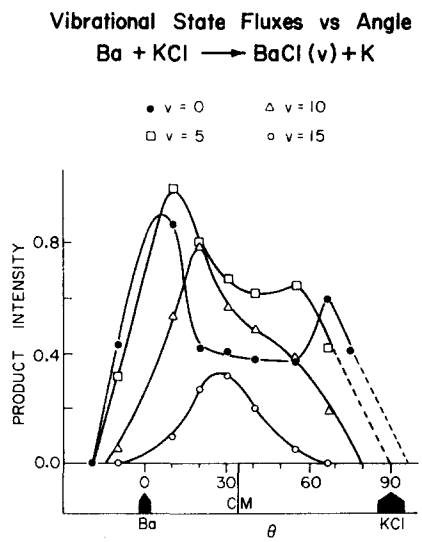

FIG. 6. Plot of the BaCl vibrational state fluxes as a function of the laboratory scattering angle θ, in a manner similar to Fig. 5.

selected vibrational levels. Figure 6 is the corresponding graph of relative vibrational fluxes, obtained by multiplying the experimental densities of Fig. 5 by the average value of v_{LAB}, as computed in the simulations just discussed. The above transformation hardly alters the distributions, and inaccuracies in the average value of v_{LAB} at a given θ have little effect. In these two figures, the shape of the angular distributions are nearly identical for both $v = 0$ and $v = 5$, but for $v = 0$ the height of the flux distribution increases compared to the density distributions. Both the $v = 0$ and $v = 5$ levels peak in the forward direction (toward the Ba beam), and both show considerable backward intensity. While $v = 5$ has the greater flux, $v = 0$ shows sharper forward and backward peaking. The $v = 10$ plot is similar to that for $v = 5$, but has a more pronounced forward–backward asymmetry, and peaks closer to the center-of-mass angle, $\theta_{c.m.}$ The flux plots (Fig. 6) for $v = 10$ and $v = 15$ both show less intensity than the density plots (Fig. 5). For each graph, $v = 15$ is lower and peaks closer to $\theta_{c.m.}$ than $v = 10$. A slight forward asymmetry remains. It appears that somewhat more BaCl products are produced in $v = 15$ than $v = 0$ at $\theta_{c.m.}$ In any case, the forward–backward peaking apparent for $v = 0$ is no longer seen for $v = 15$.

Figure 7 presents vibrational state fluxes at various laboratory angles. The most notable asymmetry is the enhanced intensity for low and moderate vibrational levels at 10° compared to 55°, its backward compliment with respect to $\theta_{c.m.}$

The BaCl excitation spectrum for the total reaction has also been taken by making the reaction and excitation zones coincide. The method of analysis is the same as before, without conversion of density to flux, and the results are similar to those for $\theta = 30°$ shown in Fig. 7.

For one run it was possible to measure a very crude angular distribution of the potassium atom product. This is the first instance for which LIF has detected

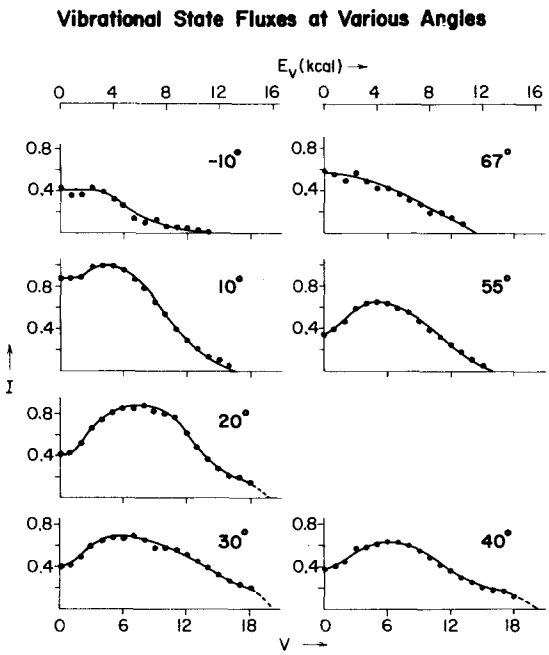

FIG. 7. Graph of the BaCl product fluxes at various laboratory scattering angles as a function of the vibrational level. The three pairs of angles, (−10°, 67°), (10°, 55°), and (30°, 40°) are approximately symmetrically placed about $\theta_{c.m.} = 34°$, and these graphs are shown side by side. The intensity scale is the same as Fig. 6 and a scale for the vibrational energy in kcal/mole is placed at the top of the figure. The solid circles are the experimental data, which are connected by a curve to aid visualization.

both reaction products. Rather than using the K atom D_1 and D_2 resonance lines that lie in the red, we chose to excite the 4044 Å transition (K $4s$ − K $5p$) using the dye PBBO. While all K atoms produced can be pumped, nevertheless their detection proves very difficult because (1) the K atoms have a much smaller spatial density than BaCl, (2) the K $4s$ − K $5p$ transition is rather weak, and (3) only about 17% of the radiative decay of the K $5p$ state occurs in the visible. Consequently, the observed angular distribution is not of high quality, but it suffices to show forward and backward intensity, with the backward peak larger than the forward. This preferential backward scattering is in agreement with our previous observation of preferential forward scattering of the BaCl product. The K atom distribution is wider than the BaCl distribution and extends beyond the range for which angular measurements can be made with the present apparatus. This result is expected since the K atom is the lighter product and has the higher velocity, i.e., $m_K u_K = m_{BaCl} u_{BaCl}$.

One previous attempt has been made by S. C. Khandelwal[13] to measure an angular distribution for Reaction (1) independent of the velocities or internal states of the products. He used a "methanated" hot wire without mass selection as his detector. Because BaCl and K, with ionization potentials of ~4.8 eV[14] and 4.3 eV are both probably detected but to unknown different extents, we are unable to reinterpret his data to make any meaningful comparison with the present work.

IV. DISCUSSION

The experimental study of the dynamics of bimolecular reactions has proceeded in the past from two different viewpoints, based on the interpretation of two different data sets. In one case, angular distribution data are used to provide a "clock" for measuring the lifetime of the collision complex. This permits conclusions to be reached whether the reaction mechanism proceeds through a persistent complex long lived with respect to rotation (sticky collision), or through a more direct scattering process (such as spectator stripping) in which the reactants rapidly rearrange to form products that quickly separate from one another. In the other case, internal state populations are used to indicate a probable reaction mechanism by comparing the experimental distributions with those predicted from some model. In particular, the internal state distributions may be compared with those calculated from statistical models in order to determine whether the collision complex lives long enough to achieve an equipartition of its energy among the degrees of freedom of the complex.

It should be noted from the above that one can distinguish two characteristic time constants of the collision complex, one controlling the angular distribution of the products, the other controlling the energy distribution. Moreover, these two time constants need not be equal. In previous experimental studies of reaction dynamics, it has not been possible to investigate both characteristics because angular and internal state distributions have not been measured simultaneously. The present study provides a first step in this direction in which the angular distribution of individual internal states is measured. By this means a most interesting relation between angular and internal state product distributions results for the Ba + KCl reaction.

The data most readily obtained from a LIF study of a reaction is the partitioning of energy. Table I presents a comparison of the experimental internal state distributions obtained from the BaCl excitation spectrum for the total reaction with those calculated from phase space theory (PST).[11,15,16] Phase space theory is a statistical treatment in which the probability for breakup of the reaction complex into certain product states is simply proportional to the number of ways (density of states) for this to occur, provided energy and angular momentum are conserved. In Table I, the

TABLE I. Energy partitioning (kcal/mole).

	Phase space theory		Experiment			
v	N_{VIB}(%)	T_{ROT}(°K)	N_{VIB}(%)	T_{ROT}(°K)	$\bar{E}_{INT}$	$\bar{E}_{TR}$
0	10.0	4600	4.4	5200	10.4	3.4
5	7.5	3300	6.7	4300	12.6	1.5
10	4.8	2300	6.0	3400	14.8	0.6
15	2.4	1200	4.0	2500	17.0	0
20	0.4	300	0.0	···	···	···

	Theory	Experiment	Simulation
$\bar{E}_{VIB}$	4.2	6.5	
$\bar{E}_{ROT}$	6.7	7.5	
$\bar{E}_{TRANS}$	5.5	2.4	1.2

theoretical rotational temperatures are chosen so that the Boltzmann distribution peaks at the same value of J as calculated from PST (strictly speaking, PST predicts a non-Boltzmann distribution). On comparison with the admittedly crude experimental values of T_{ROT}, Table I shows that the theoretical values of T_{ROT} are too low for all v. In particular, the $v=15$ value for T_{ROT} is so low that PST predicts the appearance of an unobserved sharp band head. Nevertheless, the average rotational energy found from PST does not differ dramatically from experiment.

The contrast between PST and experiment becomes more marked when the BaCl vibrational distribution is examined. The gap between the experimental and theoretical average vibrational energy is about 2.5 kcal/mole, causing PST to overestimate the average translational energy found from experiment. When the form of the vibrational distribution is considered, it is seen that PST predicts a smooth falloff from $v=0$, as would be expected from any statistical theory because of the higher density of states associated with lower v levels. On the other hand, experiment shows that the BaCl vibrational distribution peaks around $v=7$. Consequently, we conclude at once that a statistical treatment of the energy partitioning for the Ba + KCl reaction will be inadequate to explain the reaction dynamics. Hence, the lifetime of the reaction complex does not permit energy equilibration before product separation.

Estimates of the average product translational energy for various BaCl vibrational levels are also given in Table I. These values are taken from the angular distribution simulations shown in Fig. 4. An interesting effect is apparent from this table of translational energies, especially for the higher vibrational levels. As the amount of internal energy increases, the amount of translational energy does not decrease by a corresponding amount. This indicates that the higher vibrational levels are produced mainly in collisions of above-average reactant energy, either translational energy or KCl internal energy. Table I also lists two possible experimental values for the average barycentric translational energy of all products formed. The "simulation" value is derived from the angular distribution simulations, while the "experiment" value is derived from the difference between the average total available energy (collision energy, KCl internal energy, and reaction exothermicity) and the average BaCl internal energy. Phase space theory clearly overestimates the amount of translational energy, compared to either value. The simulation value of the average translational energy can also be used to estimate the BaCl bond energy. This gives a value of 109 kcal/mole, compared to 110 ± 3 kcal/mole obtained by previous work in this laboratory using single-collision chemiluminescence and LIF methods.[4]

We consider next the angular distributions shown in Fig. 5. Clearly, the higher vibrational levels have less energy available for translation and such BaCl products are constrained to lie in the region around the center of mass. The results also indicate that the large amount of rotational energy found in the higher vibrational levels near $\theta_{c.m.}$ has not been redistributed into translational energy at larger angles. The contrary is true for low vibrational levels. Rotational temperatures for $v=0$ drop off sharply at angles distant from the center of mass: 5200 °K at 20°; 4000 °K at 10°; and 1600 °K at −10°. Thus the higher translational energy required at angles distant from $\theta_{c.m.}$ is borrowed from both vibration and rotation.

A second general feature of Fig. 5 is the extent of both forward and backward scattering, with forward predominating, for all vibrational levels. Indeed, the forward-to-backward ratio is constant within a few percent for $v=0$ to $v=12$, and has the value 58:42.[17] The simulated angular distributions indicate an osculating complex that only lives roughly one-half of a rotational period. A second possibility is that the reaction occurs by two separate pathways, such as forward stripping and backward rebound mechanisms. The LIF technique provides additional information to rule out this possibility, since one would expect two different processes to show different internal energy distributions. For example, the greater impact parameter of a stripping collision should produce more rotationally excited products. On the other hand, the head-on nature of a rebound collision might result in greater vibrational excitation. Since the rotational temperatures show a remarkable angular symmetry for $v=0$ and the angular distributions show a consistent 58% forward fraction for different vibrational levels, a single, osculating complex mechanism appears to be the best description.

An approximate lifetime for this complex can be obtained as follows. Let μ be the reduced mass of the collision partners, b the impact parameter, and v_{REL} the magnitude of the relative velocity. Then the time of a rotational period of a complex is calculated from the expression

$$t_{ROT} = 2\pi I/L \ , \tag{10}$$

where

$$I = \mu b^2 \tag{11}$$

is the moment of inertia and

$$L = \mu v_{REL} b \tag{12}$$

is the angular momentum. We estimate the impact parameter b from the cross section σ by the relation

$$b = (\sigma/\pi)^{1/2} \ . \tag{13}$$

Substitution of Eqs. (11)–(13) into Eq. (10) gives for the rotational period

$$t_{ROT} = 2(\sigma\pi)^{1/2}/v_{REL} \ . \tag{14}$$

Using a rough estimate of the cross section as $\sigma = 40$ Å^2 and the average value of the relative velocity $v_{REL} = 7.5\times10^4$ cm/sec, we estimate $t_{ROT} = 3\times10^{-12}$ sec. Thus, the energy of an average KClBa complex has not become equilibrated in the typical lifetime of 1.5×10^{-12} sec.

The appearance of an osculating complex for Reaction (1) is not surprising compared to previous alkali atom–

alkali halide exchange reactions.[6,7] The similar metallic natures of alkalies and alkaline earths suggest both reactive systems should have a deep well for the complex, as found for the alkalies.[7] The exothermicity of Reaction (1) is also in the range of previously observed osculating complexes. The direct reaction Li + KF is exothermic by $\Delta H \approx -20$ kcal/mole.[7] For the osculating complexes Cs + TlCl, $\Delta H \approx -17$ kcal/mole,[6] and Li + KCl, $\Delta H \approx -11$ kcal/mole.[7] The persistent complex Cs + RbCl has a ΔH of -6 kcal/mole.[6] Reaction (1) is exothermic by $\Delta H = -9.5 \pm 3.5$ kcal/mole and fits into this trend.

A rough characterization of the potential surface for this reaction may also be made. As reactants approach, an electron jump occurs, according to the familiar harpoon model,[1] forming an ionic intermediate of the configuration Ba^+Cl^-K. Using an electron affinity of 29.3 kcal/mole for KCl,[18] the crossing point occurs at a separation of roughly 3.7 Å. This would predict a cross section for complex formation of ~40 Å^2. The Coulomb attraction produces an energy well for the complex, which by analogy to the similar alkali metal systems[7] would be roughly 15 kcal/mole.

Alternatively, RRKM theory[19] may be used to give an independent estimate of the well depth from the expression

$$\tau = \tau_0 \{[\mathcal{E}' + \mathfrak{D}' - (I^*/I)\langle B'\rangle]/(\mathcal{E}' - \langle B'\rangle)\}^{n+1} . \qquad (15)$$

Here τ is the lifetime of the complex (1.5×10^{-12} sec); τ_0 is a representative vibrational period (1.7×10^{-13} sec); $\mathcal{E}'$ is the energy available to the products (16.4 kcal/mole); $\mathfrak{D}'$ is the well depth (which is to be found); I^*/I (estimated to be 2.8) is the ratio of the moments of inertia of the transition state, taken to be the peak of the exit centrifugal barrier to the complex; $\langle B'\rangle$ is the mean centrifugal energy at the transition state[16] (1.77 kcal/mole); and n is the number of degrees of freedom for the complex ($n = 2$ for the loose complex assumed here). In this manner we obtain an estimate of the well depth of 18 kcal/mole, in satisfactory agreement with the well depth obtained by analogy to the alkali systems.

The present results indicate that the available energy has not equilibrated itself in accord with phase space predictions in the short lifetime of an osculating complex. For such short-lived complexes, the average back-scattered product comes from a longer-lived intermediate than those forward scattered. However, the LIF angular distribution data show no discernible differences in forward and backward internal energy distributions. This lack of greater energy equipartitioning in the backward direction suggests that energy equilibration has not proceeded significantly within one rotational period. Thus, statistical theories such as RRKM which assume equilibration of energy among all degrees of freedom on the time scale of a vibrational period (~10^{-13} sec) may not apply even for some persistent complexes with lifetimes of several rotational periods, at least for small systems.

The measurement of angular distributions of product internal states for the Ba + KCl reaction, via LIF, has provided a detailed picture of the behavior of a short-lived complex. Despite the difficulty encountered in coordinate transformations caused by the lack of knowledge of velocities, the LIF method offers several interesting opportunities for future angular distributions. One could characterize the product internal energy distributions from a series of different complexes having different lifetimes. A second interesting prospect suggested by this work involves differences in angular distributions of individual rotational states. Experiments to obtain such details using the LIF technique, while difficult, now appear feasible.

ACKNOWLEDGMENTS

We are grateful to P. J. Dagdigian for his construction of the scattering apparatus, to R. K. Sander for assistance with the laser system, and to F. Engelke for many useful discussions and help in early experiments. This work is supported by the National Science Foundation.

[1] R. D. Levine and R. B. Bernstein, *Molecular Reaction Dynamics* (Oxford U.P., New York, 1974).
[2] R. N. Zare and P. J. Dagdigian, Science **185**, 739 (1974).
[3] S. H. Bauer and R. F. Porter, in *Molten Salt Chemistry*, edited by M. Blander (Interscience, New York, 1964), p. 607.
[4] P. J. Dagdigian and R. N. Zare, J. Chem. Phys. **61**, 2464 (1974).
[5] T. P. Schafer, P. E. Siska, J. M. Parson, F. P. Tully, Y. C. Wong, and Y. T. Lee, J. Chem. Phys. **53**, 3385 (1970).
[6] W. B. Miller, S. A. Safron, and D. R. Herschbach, Discuss. Faraday Soc. **44**, 108 (1967); G. A. Fisk, J. D. McDonald, and D. R. Herschbach, *ibid.*, p. 228.
[7] G. H. Kwei, A. B. Lees, and J. A. Silver, J. Chem. Phys. **55**, 456 (1971); A. B. Lees and G. H. Kwei, J. Chem. Phys. **58**, 1710 (1973).
[8] Our thanks for this dye to C. S. Angadiyavar and R. Srinivasan, IBM Watson Research Center, Yorktown Heights, N.Y.
[9] R. E. Drullinger and R. N. Zare, J. Chem. Phys. **51**, 5532 (1969); *ibid.* **59**, 4225 (1973).
[10] H. W. Cruse, P. J. Dagdigian, and R. N. Zare, Faraday Discuss. Chem. Soc. **55**, 277 (1973).
[11] P. J. Dagdigian, H. W. Cruse, A. Schultz, and R. N. Zare, J. Chem. Phys. **61**, 4450 (1974).
[12] R. Wolfgang and R. J. Cross, Jr., J. Phys. Chem. **73**, 743 (1969); T. T. Warnock and R. B. Bernstein, J. Chem. Phys. **49**, 1878 (1968).
[13] S. C. Khandelwal, Ph. D. thesis, Univ. of Arizona, Tucson, 1974.
[14] K. S. Krasnov, Teplofiz. Vys. Temp. **3**, 927 (1965) [High Temp. **3**, 927 (1965)].
[15] P. Pechukas, J. C. Light, and C. Rankin, J. Chem. Phys. **44**, 794 (1966).
[16] Polarizabilities α and dipole moments μ used for phase space calculations are as follows: Ba $\alpha = 43.6$ Å^3; K $\alpha = 45.2$ Å^3, S. A. Adelman and A. Szabo, J. Chem. Phys. **58**, 687 (1973); KCl $\mu = 10.5$ D, C. A. Lee, R. D. Carlson, B. P. Fabricand, and I. I. Rabi, Phys. Rev. **91**, 1395 (1953); BaCl $\alpha = 14.8$ Å^3, KCl $\alpha = 4.6$ Å^3, by adding ionic polarizabilities from K. S. Krasnov and N. V. Karaseva, Opt. Spectrosc. **19**, 14 (1965) and C. P. Smyth, *Dielectric Behavior and Structure* (McGraw-Hill, New York, 1955); BaCl $\mu = 8.8$ D, crudely estimated by multiplying the ionic dipole er, $r = 2.7$ Å (Ref. 10), by the percent ionic bonding derived from electronegativities by L. Pauling, *College Chemistry* (Freeman, San Francisco, 1964), 3rd ed., p. 280.

[17]For higher vibrational levels, the forward percentage is known less accurately, but appears to increase. This may be due to the shorter lifetimes of complexes formed in higher energy collisions, which appear to decompose preferentially to the higher levels.

[18]H. Ebinghaus, Z. Naturforsch Teil A **19**, 727 (1964).
[19]W. B. Miller, S. A. Safron, and D. R. Herschbach, J. Chem. Phys. **56**, 3581 (1972).